ELSEVIER

Physica C 369 (2002) 335–338

PHYSICA C

www.elsevier.com/locate/physc

STM imaging of vortex configurations in films of a-Mo_3Ge through a Au layer

G.J.C. van Baarle*, A.M. Troianovski, P.H. Kes, J. Aarts

Kamerlingh Onnes Laboratory, Leiden University, 2300RA Leiden, The Netherlands

Abstract

We report on visualization of the vortex configuration in thin films (50 nm) of amorphous (a-) Mo_3Ge by means of scanning tunnelling spectroscopy (STS) at 4.2 K. We prepared the Mo_3Ge films by rf-sputter deposition. To avoid oxidation during mounting of the film in the scanning tunnelling microscopy (STM), we deposited a thin (typically 3 nm) protecting Au layer immediately after deposition of the Mo_3Ge layer. STM investigation showed the surface of this Au layer to be very smooth. STS in zero-field showed a proximity-induced gap everywhere on the surface and vortex lattices could be imaged in grid-mode in fields up to 0.6 T.

Keywords: Vortex imaging; STM; STS; Superconductivity

1. Introduction

Scanning tunnelling microscopy (STM) is one of the tools available to image vortex structures. However, research until now has been limited to crystals which can be cleaved and are not sensitive to oxidation. Well-known examples are $NbSe_2$ [1, 2], YBCO [3] and BSCCO [4] crystals. Especially, no direct imaging of vortex lattices in thin films was reported, even though that would yield a wealth of information on e.g. vortex configurations in artificial structures. A major obstacle is the fact that it is difficult to grow superconducting films with a surface both smooth and clean enough to perform STM investigations. For example, in the case of a-Mo_3Ge, to be discussed below, we found it impossible to perform spectroscopy on the bare surface, apparently due to the formation of an insulating top layer during mounting of the sample.

2. The samples

We chose a-Mo_3Ge as superconducting material because of the extremely flat surface characteristic of amorphous films, in contrast to e.g. a (polycrystalline) Nb surface, which shows height variations of several nm over distances of the typical grain size (10 nm). Atomic force microscopy (AFM) investigation of a freshly sputtered Mo_3Ge film showed the surface to have a roughness <0.4 nm over the scan range of 0.5 μm. Moreover, the low intrinsic pinning properties, the superconducting transition temperature T_c of 6.5 K and the upper

* Corresponding author.
E-mail address: baarle@phys.leidenuniv.nl (G.J.C. van Baarle).

0921-4534/01/$ - see front matter
PII: S0921-4534(01)01271-0

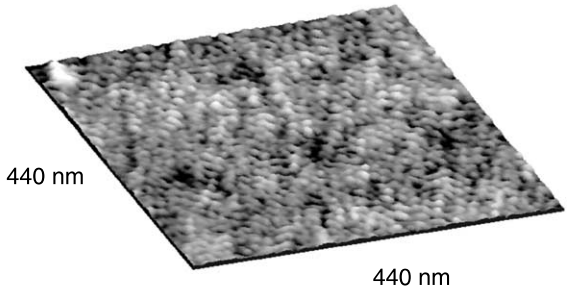

Fig. 1. STM topography image of a 440×440 nm^2 Mo_3Ge film with a 6 nm Au layer taken at 4.2 K and $V_b = 4.0$ mV. From black to white corresponds to 3 nm height difference.

critical field at 4.2 K of 6 T make a-Mo_3Ge a suitable candidate for use in tailored samples. The films were rf-sputtered from a composite Mo/Ge target in Ar atmosphere. To avoid crystallization the temperature of the silicon substrate was kept close to room temperature during deposition. Immediately after the deposition of the Mo_3Ge a 6 nm Au layer was sputtered on the surface. This yielded a rather flat, closed protection layer with a maximum height variation of the surface of around 3 nm on a 440 nm $\times$ 440 nm scan. A typical topography image is shown in Fig. 1. This image was measured at 4.2 K with the bias voltage V_b well above the gap.

Our STM-head is directly immersed in the liquid Helium, so a constant temperature is ensured. At 4.2 K we were able to measure a gap everywhere on the surface. At this temperature, thermal excitations of quasiparticles will be present, resulting in a non-zero density of states (DOS) in the gap region and reduced quasiparticle peaks. In Fig. 2 a typical measurement of the DOS is shown (bright line), together with the theoretical BCS curve (dashed line). The BCS-curve reaches zero at zero bias. The differences between the experimental data and the calculated curve, in particular the broader quasiparticle peaks of the BCS curve and the zero DOS at zero bias, can partly be explained by the fact that we did not take into account the changed origin of the pair potential for proximity induced superconductivity and bound states due to the Au grains [5]. Within the noise, the shape of the gap did not show large variations over the sample surface.

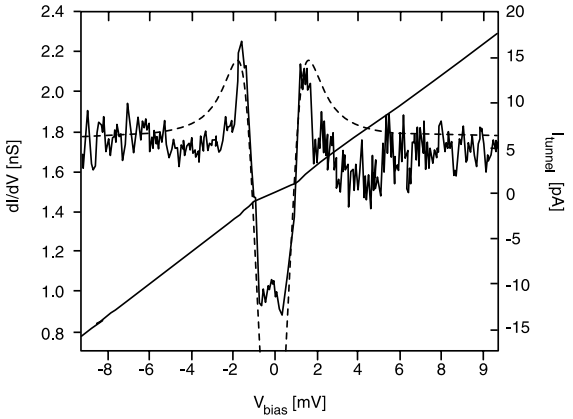

Fig. 2. Example of an I–V curve (dark curve, right-hand axis) and a numerically derived dI/dV spectrum (light curve, left-hand axis). Dashed curve gives a BCS fit for the DOS ($T_c = 6.5$ K and $T = 4.2$ K). Note the non-zero slope of the I–V curve at low bias voltage due to thermal excitations and the proximity-origin of the gap. The dotted curve gives a dI/dV spectrum measured at a vortex core.

3. Experimental

Upon applying a magnetic field, vortices enter the sample, which results in local suppression of the gap. To obtain a spatial image of this behavior, several techniques can be used. First one can obtain an image by scanning the sample choosing $V_b < \Delta$ and keeping the tip-sample distance constant. The tunnel current value then is a measure for the presence of the gap. For our samples, this method did not yield good results because of the small size of the gap which restricts us to low V_b and low currents; together with the residual roughness of the surface this makes scanning difficult. Moreover, the non-zero DOS in the gap region reduces the contrast. The second possibility is to add a small modulation voltage to V_b which is adjusted at Δ. Via lock-in detection this will result in mapping the local DOS at Δ which is large in case of presence of the quasiparticle peaks. Again, due to the high temperature relative to T_c and the noise, this did not yield clear images. The third method, measuring the full I–V curves on a 64×64 point grid yielded good results. An example of such a curve measured in zero field is given in Fig. 2, together with its numerically computed dI/dV.

dI/dV curves measured on a vortex core appeared to be flat, particularly the gap region is featureless. For every curve we compute the slope at high V_b (well above Δ) and around zero bias. The ratio of these numbers provides information about the presence of the gap. An advantage of this method is that the noise can be reduced by averaging more I–V curves measured at the same point due to the good stability of the tunnel junction. The price to be paid is the low speed of the measurement (depending on the amount of curves taken, but typically more than 30 min for each 64×64 image). The results shown below are obtained with this method.

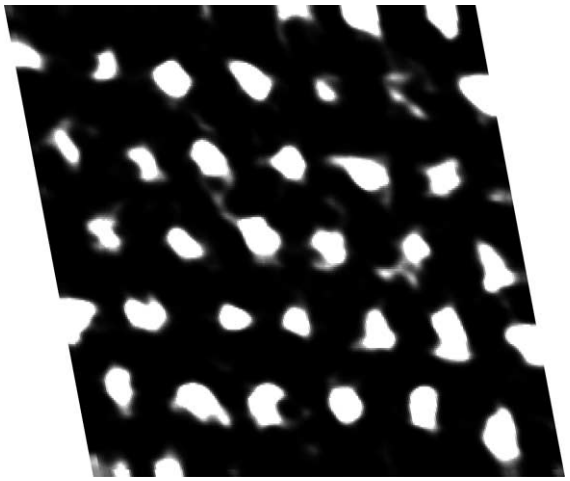

Fig. 3. Vortex configuration for a magnetic field of 0.4 T imaged on the sample from Fig. 1 by the method discussed in the text. Scan size: 440×440 nm^2.

4. Results

In Fig. 3 we show a typical image with size of 440 nm $\times$ 440 nm measured at 4.2 K and with applied magnetic field of 0.4 T on a 50 nm thick Mo_3Ge film covered with 6 nm Au. The I–V curves are taken simultaneously with the topographical data shown in Fig. 1 by interrupting the scanning at specific positions, and measuring one ore more I–V curves. To correct the non-orthogonality of the x- and y-scan direction, we sheared the image according to a calibration based on imaging the atomic structure of a $NbSe_2$ surface. The regularly

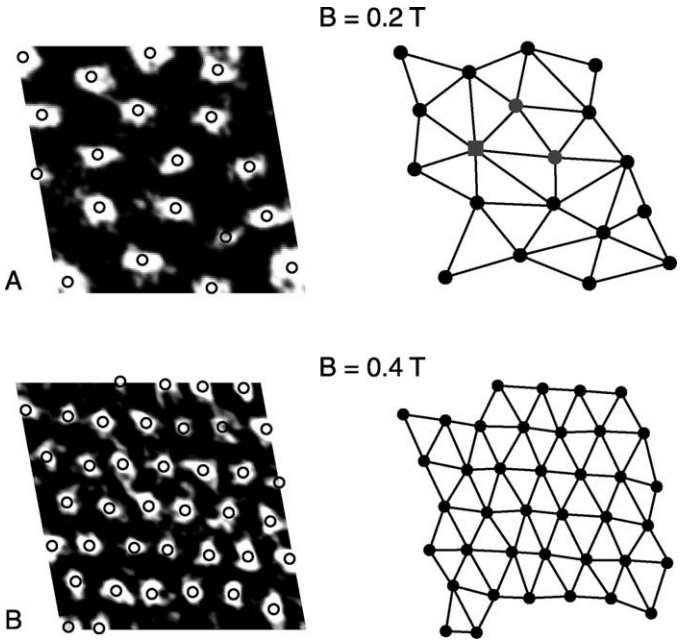

Fig. 4. Vortex configuration at 0.2 and 0.4 T together with their triangulations. Vortices with only five or seven nearest neighbors are marked by grey circles and squares respectively. The scanned area of both pictures is 440×440 nm^2.

placed bright spots show the characteristics of a vortex structure: the magnetic flux density of 0.4 T corresponds to an inter-vortex distance $a_0 = 77.3$ nm, which very well agrees with our data yielding $a_0 \approx 77$ nm. Moreover, a hexagonal lattice is clearly observed. Such hexagonal lattices could be observed for magnetic flux densities up to 0.6 T. On reducing the magnetic field we observe the expected reduction in vortex density as is shown in Fig. 4. Furthermore we see that on reducing the magnetic flux density, the lattice becomes less regular.

In Fig. 4 we also show a triangulation of the vortex configuration, from which is clearly seen that the amount of defects increases with decreasing field. This can be attributed to the competition between the elastic interactions in the vortex lattice and the single vortex pinning force due to impurities in the sample. For these weakly pinning materials, the ratio R_c/a_0 (vortex lattice correlation length in units of vortex distance) increases more or less linearly with the magnetic field at low reduced field $b = B/B_{c2}$. For the parameters of the experiment, $T/T_c = 0.6$ and $b = 0.07$, the value of R_c/a_0 is of order of 5 or less, and defects can still be expected. Experiments to probe these correlations at higher fields need increased grid resolution and scan size and are currently under development.

References

[1] A. Troyanovskii, J. Aarts, P.H. Kes, Nature 399 (1999) 665.
[2] H.F. Hess, R.B. Robinson, R.C. Dynes, J.M. Valles Jr., J.V. Waszczak, Phys. Rev. Lett. 62 (1989) 214.
[3] I. Maggio-Aprile, Ch. Renner, A. Erb, E. Walker, Ø. Fischer, Phys. Rev. Lett. 75 (1995) 2754.
[4] Ch. Renner, B. Revaz, K. Kadowaki, I. Maggio-Aprile, Ø. Fischer, Phys. Rev. Lett. 80 (1998) 3606.
[5] A.D. Truscott, R.C. Dynes, L.F. Schneemeyer, Phys. Rev. Lett. 5 (1999) 1014.